



Numerical evaluation of transient deflection and frequency responses of sandwich shell structure using higher order theory and different mechanical loadings

Pankaj V. Katariya¹ · Subrata K. Panda¹

Received: 20 August 2018 / Accepted: 26 September 2018 / Published online: 3 October 2018
© Springer-Verlag London Ltd., part of Springer Nature 2018

Abstract

The static deflection, frequency and transient responses of the layered sandwich shell (flat/curved) structure computed under the different types of mechanical loading. The higher order polynomial kinematic type of mid-plane kinematics is derived for the mathematical modeling and subsequent numerical analysis. A suitable home-made code is prepared in MATLAB for the computation of deflection (static and dynamic) parameter using the proposed mathematical model. Furthermore, the numerical solution accuracy has been verified by comparing the numerical output with those available published data including the convergence test as a priori. In addition, the influences of the variable design parameters (span-to-thickness ratios, curvature ratios, aspect ratios, core-to-face thickness ratios, lamination configurations, shell configurations, and support conditions) on the deflection, frequency, and the transient values are computed extensively and the inferences provided in details.

Keywords Sandwich shell · Newmark integration scheme · HSDT · Deflection · Frequency · Transient · MATLAB

1 Introduction

In the present scenario, the major concern of the high-performance engineering industries like aerospace, aeronautical, automobile, marine etc. is to reduce the weight without compromising the strength by adopting the advanced materials. The fibre-reinforced composite and sandwich components are the suitable alternative for these industries over the available monolithic metallic materials because of their variable stiffness, unmatched strength including the good damage tolerance. The sandwich structure is made of by placing the thick lightweight core (high density) in between the thin laminated facesheets. These sandwich configurations are widely acknowledged in the main stream structural engineering field due to their unparalleled stiffness and impact strength. In general, the bending load is transferred by the sandwich facesheets, whereas the core majorly helps

in resisting the shear and the normal loading. All the possible design concepts generally followed in the composite laminates are often adopted for the sandwich construction. Hence, it is important to analyse the sandwich structural behaviour under the different conditions (loading and environment) without negotiating the accuracy and minimal cost. However, the design, fabrication and analysis constantly associated with some major complexities. In addition, these structures or structural members are being operated under the influences of different distinct or the combined loading and experiences variable scale of deformation due to the dynamic loading. Therefore, the mathematical modeling of these structures requires adequate precision to evaluate the transverse shear deformation effects. Therefore, the modeling and analysis steps are needed a comprehensive understanding related to the influential parameters for the accurate estimation of the desired output.

The researchers have already adopted various modeling approaches including the solution techniques (analytical, numerical, and simulation) for the evaluation of layered composite or the sandwich structural components in the past. Furthermore, the structural design associated with influential output (deflection, frequency, and transient) of the layered and sandwich structures are generally examined [1, 2] using the different types of shear deformation kinematics to mimic

✉ Subrata K. Panda
call2subrat@gmail.com; pandask@nitrrkl.ac.in

Pankaj V. Katariya
pk.pankajkatariya@gmail.com

¹ Department of Mechanical Engineering, NIT Rourkela, Rourkela, Odisha 769008, India

the mid-plane deformations via the classical laminate plate theory (CLPT), normal deformation (ND), first-order shear deformation theory (FSDT), higher order shear deformation theory (HSDT), third-order shear deformation theory (TSDT) and refined theories etc. To establish the requirements of the present analysis, a brief review of some prominent and substantial contributions in the past are discussed in the following lines what follows.

The layered composite/sandwich plate/beam like structure and corresponding responses (vibration, deflection, and transient) are examined [3–9] using Mindlin's or the HSDT kinematics including von-Karman nonlinear strain for the inclusion of large deformation characteristics. Furthermore, the dynamic deflections of the skew sandwich plate structure under influence of thermomechanical combined load is investigated [10] using various kinematic theories (FSDT and HSDT). Reddy's higher order mid-plane kinematic model including the finite-element method (FEM) are adopted [11, 12] predict the transient deflection parameter of the flat sandwich/composite structure. In addition, the FSDT and the HSDT mid-plane deformation kinematics are adopted [13] to evaluate the time-dependent responses of various structures (composite and sandwich) using the radial basis functions in a pseudo-spectral framework in conjunction with Kansa technique. The geometrically nonlinear bending and eigenvalues of the sandwich flat structure are predicted [14] using the higher order finite-element (FE) model in association with von-Karman strain. Similarly, the generalized differential quadrature (GDQ) technique in the framework of the layerwise kinematics are adopted [15] to model the sandwich plate structure for the prediction of the static and the dynamic deflections. Subsequently, Reddy's higher order polynomial type of mid-plane deformation in conjunction with FEM steps [16, 17] utilized to investigate the effect of internal debonding between the layers on the time-dependent responses of the laminated/sandwich structure. Similarly, the layerwise theory in conjunction with Reddy's kinematic model [18] for the free vibration frequency and transient responses of the composite and sandwich structural components. The 3D FEM steps are adopted [19] to model and predict the delamination of the Spar Wingskin Joints made up of graphite fibre-reinforced plastic (GFRP) composite under the uniformly distributed transverse loading. Furthermore, the nonuniform rational B-spline (NURBS) technique is adopted to compute the eigenvalues (frequency and critical buckling load) of the composite and the functionally graded (FG) structures [20, 21] using Reissner–Mindlin plate modeling approach. Likewise, an equivalent layerwise approach in conjunction with the local GDQ methods are adopted to model the FG sandwich/composite shell structures to predict the corresponding transverse bending and free vibration frequencies [22–24]. Moreover, the different kinematic theories (first-, second-, and third-order shear deformation)

are undertaken to model and predict the effect of delamination on the responses of the sandwich structural components [25, 26]. The structural responses (static deflection and transient) of variable structural form, i.e., layered composite, graded carbon nanotubes, sandwich nanoplate and the hybrid smart structure are investigated [27–35] using the available numerical techniques (finite integral transform method, differential curvature method, differential quadrature, DQ; and harmonic differential quadrature, HDQ) and subsequent kinematic polynomials (Mindlin's plate theory, refined zigzag theory, RZT; sinusoidal shear deformation theory, SSDT; FSDT and CLPT). Similarly, the structural responses (transverse deflection, eigenfrequency and buckling load) of the isotropic, layered composite and FG sandwich structures are computed [36–55] via different higher order and hyperbolic shear deformation polynomial kinematic theories including the mid-plane stretching effect. In addition, the deflection and stress values of the skew sandwich shell panel is investigated [56] using the higher order mid-plane kinematics including the effect of geometrical large deformations.

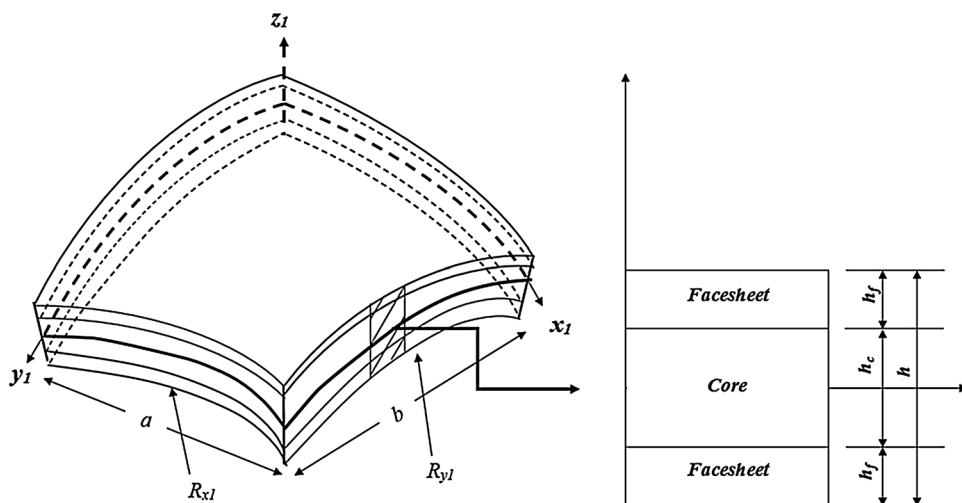
The inclusive review discussed in the above lines indicate the available knowledge gap in the present domain regarding the influence of the static and dynamic types of mechanical loading on the deflection values including the eigenvalues (free vibration frequency parameter) of the sandwich panel structure. Hence, a higher order polynomial kinematic theory has been adopted to model the sandwich structural panel including the different geometrical configurations (flat, single and doubly curved panel) for the computation of the related structural responses (transverse static and dynamic deflection and frequency) numerically. For the computation of relevant responses, an own home-made specialized MATLAB code is derived to predict the same using the derived model. Furthermore, the relevance of the derived numerical model for the computation of results is established with adequate comparison and convergence check. Finally, the influential parameter associated with geometry and dimension, i.e., the curvature ratios (R/a), the aspect ratios (alb), the core-to-face thickness ratios (h_c/h_f), the stacking sequences and the edge support conditions on the panel (flat/curved) responses (deflection, frequency and transient) have been explored extensively via solving different kind of numerical examples.

2 Modeling

2.1 Basic assumptions

The details regarding the assumed sandwich shell panel model including the curvature (one or two) along the axes are presented in Fig. 1. In general, sandwich structural panel consisting two laminated stiff layers (facings) and a soft layer (core) in between the middle of the facings.

Fig. 1 Geometry of the sandwich shell structure



For the numerical analysis purpose a few relevant assumptions are considered and presented in the following points:

- All the layers within facings (fibres and mortar) are perfectly bonded with each other to maintain as a single layer.
- The 3D shallow shell model reduced to a 2D model by implementing the adequate plane stress/strain conditions.
- The basic geometrical configurations are consisting of shallow curvature over a rectangular planform. Furthermore, geometrical shapes are achieved by changing the

(R_x and R_y are the radii of curvatures along the respective directions, whereas $R_{xy} = \infty$). The single/doubly curved panels are named as cylindrical panel if $R_x = R$ and $R_y = \infty$, spherical panel if $R_x = R_y = R$, elliptical panel if $R_x = R$ and $R_y = 2R$, hyperboloid panel if $R_x = R$ and $R_y = -R$, and flat if $R_x = R_y = \infty$.

2.3 Displacement field

The displacement polynomial functions at an arbitrary point (x_1, y_1, z_1) of the sandwich panel structure in the reference frame can be expressed as [56]

$$\left. \begin{aligned} u_1(x_1, y_1, z_1, t) &= u(x_1, y_1) + z_1\theta_1^*(x_1, y_1) + z_1^2\phi_1^*(x_1, y_1) + z_1^3\psi_1^*(x_1, y_1) \\ u_2(x_1, y_1, z_1, t) &= v(x_1, y_1) + z_1\theta_2^*(x_1, y_1) + z_1^2\phi_2^*(x_1, y_1) + z_1^3\psi_2^*(x_1, y_1) \\ u_3(x_1, y_1, z_1, t) &= w(x_1, y_1) + z_1\theta_3^*(x_1, y_1) \end{aligned} \right\} \tag{1}$$

curvature parameters, i.e., the flat, cylindrical, spherical, hyperboloid and elliptical panel configurations.

- The reference frame/global coordinate system is coinciding with the mid-plane of the shell structure.

2.2 Geometry description

The overall thickness of the panel structure is denoted as ‘ h ’, which is a combination of the thickness of the top and the bottom facings h_f including the core thickness ‘ h_c ’ (refer Fig. 1). Similarly, the length and the width of the panel are denoted as ‘ a ’ and ‘ b ’, respectively. The physical sandwich model is further transformed into a mathematical form for the numerical analysis purpose using the defined geometrical dimensions. In addition, the shell configurations are achieved using the principal radii of curvatures

where the individual coefficients associated with the kinematic model, i.e., u , v and w defined for the sandwich structural neutral plane along their corresponding directions (x_1, y_1, z_1) , respectively. Similarly, the rotation of normal to the mid-plane are denoted as θ_1 and θ_2 , respectively, with respect to the alternating axes. In addition, the higher order terms in the displacement field, i.e., ϕ_1, ϕ_2, ψ_1 and ψ_2 are kept in the expression (Taylor’s series) for the order of shear stress across the thickness including the thickness stretching term as ‘ θ_3 ’ and arbitrary time ‘ t ’.

2.4 Kinematic relations

The panel deformation is modeled using the following general form of linear strain–displacement relations including the curvature effect and expressed as

$$\begin{Bmatrix} \varepsilon_{x_1x_1} \\ \varepsilon_{y_1y_1} \\ \varepsilon_{z_1z_1} \\ \gamma_{\xi_{y_1z_1}} \\ \gamma_{\xi_{x_1z_1}} \\ \gamma_{x_1y_1} \end{Bmatrix} = \begin{Bmatrix} \frac{\partial u_1}{\partial x_1} + \frac{u_3}{R_{x_1}} \\ \frac{\partial u_2}{\partial y_1} + \frac{u_3}{R_{y_1}} \\ \frac{\partial u_3}{\partial z_1} \\ \frac{\partial u_2}{\partial z_1} + \frac{\partial u_3}{\partial y_1} - \frac{u_2}{R_{y_1}} \\ \frac{\partial u_1}{\partial z_1} + \frac{\partial u_3}{\partial x_1} - \frac{u_1}{R_{x_1}} \\ \frac{\partial u_1}{\partial y_1} + \frac{\partial u_2}{\partial x_1} + 2\frac{\partial u_3}{R_{x_1y_1}} \end{Bmatrix} \quad (2)$$

2.5 Constitutive relations of the individual layer

Now, the general elastic constitutive relations for the layered composite sandwich structural components of any *k*th layer of the face sheets are mathematically expressed in the local (material) coordinate system considering the stacking sequence ‘*Θ*’ of the fibre as [57]

$$\begin{Bmatrix} \sigma_{x_1x_1} \\ \sigma_{y_1y_1} \\ \sigma_{z_1z_1} \\ \sigma_{y_1z_1} \\ \sigma_{x_1z_1} \\ \sigma_{x_1y_1} \end{Bmatrix}^k = \begin{bmatrix} \bar{Q}_{11} & \bar{Q}_{12} & \bar{Q}_{13} & 0 & 0 & 0 \\ \bar{Q}_{12} & \bar{Q}_{22} & \bar{Q}_{23} & 0 & 0 & 0 \\ \bar{Q}_{13} & \bar{Q}_{23} & \bar{Q}_{33} & 0 & 0 & 0 \\ 0 & 0 & 0 & \bar{Q}_{44} & \bar{Q}_{45} & 0 \\ 0 & 0 & 0 & \bar{Q}_{54} & \bar{Q}_{55} & 0 \\ 0 & 0 & 0 & 0 & 0 & \bar{Q}_{66} \end{bmatrix}^k \begin{Bmatrix} \varepsilon_{x_1x_1} \\ \varepsilon_{y_1y_1} \\ \varepsilon_{z_1z_1} \\ \gamma_{\xi_{y_1z_1}} \\ \gamma_{\xi_{x_1z_1}} \\ \gamma_{x_1y_1} \end{Bmatrix}^k$$

or $\{\sigma_{ij}\} = [\bar{Q}_{ij}]\{\varepsilon_{ij}\}$ (3)

where $\{\sigma_{ij}\}$, $[\bar{Q}_{ij}]$ and $\{\varepsilon_{ij}\}$ are the individual tensors, i.e., stress, reduced transformed stiffness and the strain, respectively.

In addition, the stress can be represented as force vector in the following form:

$$\{F\} = [D]\{\varepsilon\}. \quad (4)$$

Furthermore, the individual components of the property matrix $[D]$ can be expressed as

$$[D] = \begin{bmatrix} A_{ij} & B_{ij} & C_{ij} & E_{ij} \\ B_{ij} & C_{ij} & E_{ij} & H_{ij} \\ C_{ij} & E_{ij} & H_{ij} & L_{ij} \\ E_{ij} & H_{ij} & L_{ij} & J_{ij} \end{bmatrix}, \quad (5)$$

where $[A_{ij}, B_{ij}, C_{ij}, E_{ij}, H_{ij}, J_{ij}, L_{ij}] = \sum_{k=1}^m \int_{z_{1k-1}}^{z_{1k}} (\bar{Q}_{ij})_k (z_1)^m dz_1$ for $(i, j=1, 2, \dots, 6)$ and $m=0, 1, 2, \dots, 6$.

2.6 Energy calculation

After the evaluation of stress and strain tensors of the individual layers/sandwich structural form, the strain energy (*U*) functional can be expressed mathematically in the following lines:

$$U = \frac{1}{2} \iint \left\{ \sum_{k=1}^N \int_{z_{1k-1}}^{z_{1k}} \{\varepsilon_{ij}\}^T \{\sigma_{ij}\} dz_1 \right\} dx_1 dy_1. \quad (6)$$

Similarly, the inertia and displacement field vectors are utilized to count the kinetic energy (*V*) functional for the sandwich shell structural form as

$$V = \frac{1}{2} \iint \left\{ \sum_{k=1}^N \int_{z_{1k-1}}^{z_{1k}} \rho^k \{\dot{d}\}^T \{\dot{d}\} dz_1 \right\} dx_1 dy_1, \quad (7)$$

where ρ and $\{\dot{d}\}$ are the mass density and the global velocity vector, respectively.

2.7 Work done

Now, the total work done (*W*) due to an externally applied mechanical load ‘*F*’ can be obtained using the generalized mathematical expressions as

$$W = \int \{d\}^T \{F\} dA. \quad (8)$$

2.8 Finite-element modeling

The FEM is an established numerical tool in the field of structural modeling and analysis for the complex geometrical and material problems with the adequate accuracy without compromising with computational cost. Hence, a nine-noded isoparametric element [58] with ten degrees of freedom per node is adopted for the current discretisation of the shell structure. The modified displacement field vector $\{\delta\}$ at any point in the mid-plane of the shell panel can be expressed mathematically adopting the FEM expressed as

$$\{\delta\} = \sum_{i=1}^9 [N_i] \{\delta_i\}, \quad (9)$$

where $\{\delta\} = [u \ v \ w \ \theta_1^* \ \theta_2^* \ \theta_3^* \ \phi_1^* \ \phi_2^* \ \psi_1^* \ \psi_2^*]^T$ is the nodal displacement vectors for the *i*th node and the corresponding interpolation functions (shape function) represented as $[N_i]$.

Now, the mid-plane strain vector can be expressed further after modifying the displacement and conceded to the following form:

$$\{\varepsilon\}_i = [B_i] \{\delta_i\}, \quad (10)$$

where $[B_i]$ is the strain–displacement relation matrix.

2.9 Governing equations and solution approach

2.9.1 Free vibration analysis

The final form of the governing equation of any free vibrated sandwich shell panel is obtained using Hamilton’s principle and expressed as

$$\delta \int_{t_1}^{t_2} (V - U)dt = 0. \tag{11}$$

Now, substituting the Eqs. (6), (7) and (9) into Eq. (11), the final form of the eigenvalue equations of the sandwich panel structure can be represented as

$$[M]\{\ddot{d}_i\} + [K]\{d_i\} = 0, \tag{12}$$

where $\{\ddot{d}_i\}$ is the acceleration, $\{d_i\}$ is the displacement. $[K]$ and $[M]$ are the stiffness and mass matrices, respectively, and can be expressed as

$$[K] = \int_A \left(\sum_{k=1}^N \int_{z_{1,k-1}}^{z_{1,k}} [B]^T [D] [B] dz_1 \right) dA \text{ and}$$

$$[M] = \int_A \left(\sum_{k=1}^N \int_{z_{1,k-1}}^{z_{1,k}} [N]^T [N] \rho dz_1 \right) dA,$$

where $[D] = \sum_{k=1}^N \int_{z_{1,k-1}}^{z_{1,k}} [T]^T [\bar{Q}] [T] dz_1$.

Furthermore, by neglecting the required matrices, the eigenvalue form of the governing equation can be defined as in Eq. (13) to obtain the natural frequency of the system and represented as

$$([K] - \omega^2[M])\Delta = 0, \tag{13}$$

where ω and Δ are the natural frequency and the corresponding eigenvector, respectively.

2.9.2 Static analysis

The final form of the governing equation for static analysis of any sandwich shell panel is obtained using variational principle and conceded as

$$\delta \Pi = \delta U - \delta W = 0, \tag{14}$$

where δ is the variational symbol and Π is the total potential energy.

Now, the equilibrium equation under the influence of the static loading is obtained by substituting Eq. (14) for Eqs. (6), (8) and (9) as follows:

$$[K]\{d\} = \{F\}. \tag{15}$$

2.9.3 Transient analysis

The time-dependent deflection responses are computed by solving the structural static equilibrium equation for a particular time ‘ t ’ including the inertia (acceleration-dependent) and damping (velocity-dependent) forces of the sandwich shell panel. The transient governing equation of equilibrium of the current system is obtained from Lagrangian equations of motion [59] and expressed as

$$[M]\{\ddot{d}\} + [C]\{\dot{d}\} + [K]\{d\} = \{F\}. \tag{16}$$

Here, the mass, damping and stiffness matrices are denoted as $[M]$, $[C]$, and $[K]$, respectively, and $\{F\}$ represents the external force vector. The acceleration, velocity, and displacement vectors are represented as \ddot{d} , \dot{d} and d , respectively.

Now, the solution is achieved by computing via the constant average acceleration technique of Newmark’s integration scheme, i.e., the transient equation of motion for the total time period of ‘ T ’ integrated for the small time steps (Δt). The integration parameters (α , δ , and a_0 – a_7) associated with the governing transient equation of motion adopted from the reference [59]. Now, the effective stiffness matrix for the time step ‘ t ’ conceded to the following form:

$$[\hat{K}] = [K] + a_0[M]. \tag{17}$$

Similarly, the successive steps followed for each time increments, i.e., $t + \Delta t$ to compute the effective load matrix and expressed as

$${}^{t+\Delta t}[\hat{F}] = {}^{t+\Delta t}[F] + [M](a_0 {}^t d + a_2 {}^t \dot{d} + a_3 {}^t \ddot{d}) + [C](a_1 {}^t d - a_4 {}^t \dot{d} + a_5 {}^t \ddot{d}). \tag{18}$$

Now, the following sets equations are solved to compute the associated displacement, acceleration, and the velocity terms of the transient motion equation:

$$[\hat{K}] {}^{t+\Delta t} d = {}^{t+\Delta t} [F]$$

$${}^{t+\Delta t} \dot{d} = a_0 ({}^{t+\Delta t} d - {}^t d) - a_2 {}^t \dot{d} - a_3 {}^t \ddot{d}$$

$${}^{t+\Delta t} \ddot{d} = {}^t \ddot{d} + a_6 {}^t \dot{d} - a_7 {}^{t+\Delta t} \ddot{d}. \tag{19}$$

3 Results and discussion

Now, the free vibration frequencies and the deflections (static and dynamic) are computed by solving the governing equations (eigenvalue and equilibrium) of the curved/flat sandwich shell panel. In this present analysis, the deflection and the transient responses are obtained under two different types of mechanical loading, i.e., uniformly distributed

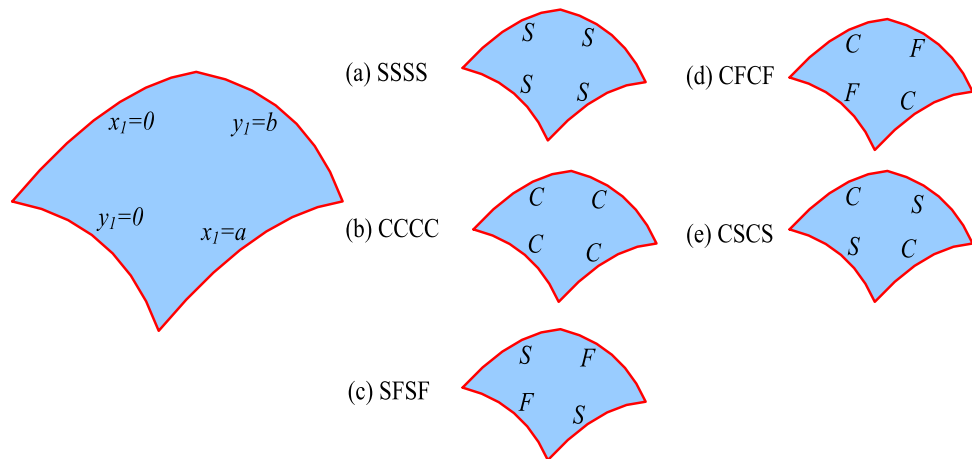
Table 1 Elastic properties of the face and core layers

M1	
Facings	$E_L = 139 \text{ GPa}; E_T = 9.86 \text{ GPa};$ $G_{LT} = G_{TT} = 5.24 \text{ GPa}; \nu_{LT} = 0.3; \rho = 1590 \text{ kg/m}^3$
Core	$E_L = 90 \text{ MPa}; G = 32 \text{ MPa};$ $\nu = 0.45; \rho = 1706 \text{ kg/m}^3$
M2	
Facings	$E_L = 19 \times 10^6 \text{ psi (131 GPa)}; E_T = 1.5 \times 10^6 \text{ psi (10.34 GPa)}; E_T = E_Z;$ $G_{LT} = G_{TZ} = 1 \times 10^6 \text{ psi (6.895 GPa)}; G_{LZ} = 0.90 \times 10^6 \text{ psi (6.205 GPa)};$ $\nu_{LT} = \nu_{LZ} = 0.22; \nu_{LT} = \nu_{TZ} = 0.49; \rho = 0.057 \text{ lb/inch}^3 (1627 \text{ kg/m}^3)$
Core	$E_L = E_T = E_Z = 2G = 1000 \text{ psi (6.89} \times 10^{-3} \text{ GPa)};$ $\nu_{LT} = \nu_{LZ} = \nu_{TZ} = 0;$ $G_{LT} = G_{LZ} = G_{TZ} = 500 \text{ psi (3.45} \times 10^{-3} \text{ GPa)};$ $\rho = 0.3403 \text{ lb/inch}^3 (97 \text{ kg/m}^3)$

loading (UDL) and sinusoidal loading (SSL), where the load intensity of SSL follow $q = q_0 \sin(\pi x_1/a) \sin(\pi y_1/b)$. To compute the final output, i.e., the static and dynamic deflections including the free vibration frequencies a suitable compute code is prepared using the above-discussed mathematical formulation in MATLAB environment. Furthermore, the finite-element solution accuracy and the convergence criteria have been checked via solving different kind of numerical examples. The sandwich facings and the core material elastic properties are taken as same as the reference [9, 10, 14] and

are provided in Table 1. In addition, the details of the edge support conditions adopted for the current analysis are shown in Fig. 2. Now, the non-dimensional parameters, i.e., the deflections and frequencies are calculated using the provided formula: $\bar{W} = 100 \times w_{\text{cen}} \times E_2 \times h^3 / q_0 \times a^4$ and $\omega = (\omega b^2 / h) \sqrt{(\rho / E_2)_f}$, respectively, unless otherwise stated elsewhere. Similarly, the time steps are adopted for the transient analysis throughout the analysis as $5 \mu\text{s}$.

Fig. 2 Details of end-support conditions



- (1) Simply support (S):
 At $x_1 = 0, a$ $v = w = \theta_2^* = \theta_3^* = \phi_2^* = \psi_2^* = 0$
 At $y_1 = 0, b$ $u = w = \theta_1^* = \theta_3^* = \phi_1^* = \psi_1^* = 0$
- (2) Clamped (C):
 At $x_1 = 0, a$ and $y_1 = 0, b$
 $u = v = w = \theta_1^* = \theta_2^* = \theta_3^* = \phi_1^* = \phi_2^* = \psi_1^* = \psi_2^* = 0$
- (3) Free (F):
 At $x_1 = 0, a$ and $y_1 = 0, b$
 $u = v = w = \theta_1^* = \theta_2^* = \theta_3^* = \phi_1^* = \phi_2^* = \psi_1^* = \psi_2^* \neq 0$

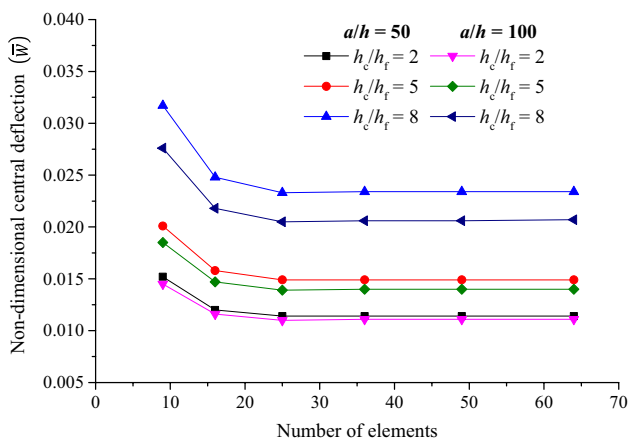


Fig. 3 Convergence study of the non-dimensional central deflection ($\bar{W} = 100wE_c h^3 / qa^4$) of SSSS square symmetric ($0^\circ/90^\circ/\text{core}/90^\circ/0^\circ$) sandwich flat panel under the UDL

First, an example is solved to obtain the non-dimensional transverse deflection values at the centre point of the structural panel including the convergence rate. For this purpose, a simply supported (SSSS) square sandwich flat panel ($0^\circ/90^\circ/\text{core}/90^\circ/0^\circ$) problem is considered. The rate convergence of deflection parameters is computed for the mechanical UDL ($q_0 = 100 \text{ N/cm}^2$) and is presented in Fig. 3 considering variable geometrical ($a/h = 50$ and 100 and, $h_c/h_f = 2, 5$ and 8) and material properties (Table 1) similar to the reference [14]. In Fig. 3, the convergence of static deflection study indicates that the deflection values are following the expected path and a (6×6) mesh adopted for the evaluation of new results.

Now, the model has been extended to check the convergence rate for the fundamental frequency parameters using the similar configuration of the plate, i.e., square, SSSS and ($0^\circ/90^\circ/\text{core}/0^\circ/90^\circ$) laminated sandwich. The obtained frequency data are tabulated in Table 2 for various mesh divisions. The geometrical and the elastic material (M2) properties (Table 1) are adopted for the analysis similar to the reference [9] values including the different span-to-thickness ratios ($a/h = 2, 4, 10, 20, 30, 40$ and 50) and core-to-face

thickness ratios ($h_c/h_f = 10$). From the tabular frequency data, it can be concluded that a (6×6) , mesh will solve the current purpose to compute the desired eigenvalue solutions.

Furthermore, a square simply supported sandwich symmetric ($0^\circ/90^\circ/\text{core}/90^\circ/0^\circ$) panel problem is solved for the different mesh divisions to establish the convergence criteria for the transient case and is plotted in Fig. 4. For the computational purpose, the SSL type of loading ($q_0 = 100 \text{ N/cm}^2$) is considered including the associated geometrical parameters ($a/h = 100$ and $h_c/h_f = 8$). The figure clearly indicates the convergence of numerical solution with respect to the mesh refinement and a (7×7) mesh is capable of computing the transient responses with appropriate accuracy for the subsequent computational purpose.

Now, the validity of the currently derived higher order sandwich panel model has been established by comparing the results with available published deflection data. In this regard, the non-dimensional central deflections are obtained for the square SSSS symmetric ($0^\circ/90^\circ/\text{core}/90^\circ/0^\circ$) sandwich flat panel using M1 material properties [14]. The deflection parameters are computed under the UDL

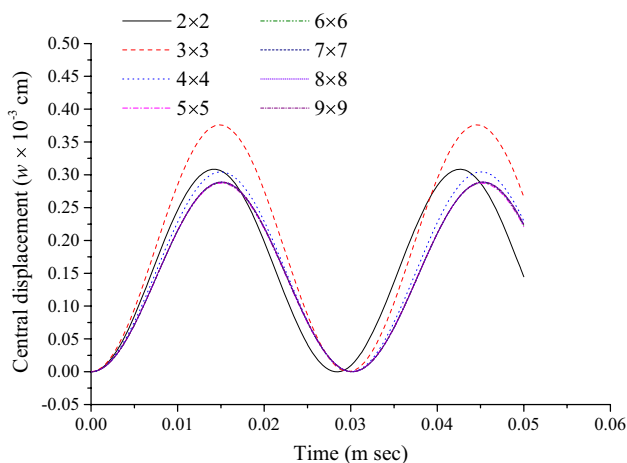


Fig. 4 Convergence behaviour of transient responses of square ($0^\circ/90^\circ/\text{core}/90^\circ/0^\circ$) sandwich flat panel under SSL ($a/h = 100$, $h_c/h_f = 8$ and SSSS)

Table 2 Convergence study of the non-dimensional fundamental frequency ($\omega = (\omega b^2/h) \sqrt{(\rho/E_2)_f}$) of simply supported square symmetric ($0^\circ/90^\circ/\text{core}/0^\circ/90^\circ$) sandwich flat panel ($h_c/h_f = 10$)

No. of elements	a/h						
	2	4	10	20	30	40	50
4	1.2422	2.1759	5.0137	8.8874	11.519	13.2263	14.352
9	1.2229	2.1561	4.9802	8.8157	11.3942	13.0362	14.0896
16	1.2178	2.1518	4.975	8.8062	11.378	13.0112	14.0537
25	1.2159	2.1501	4.9735	8.8039	11.3745	13.0057	14.0456
36	1.2151	2.1494	4.9729	8.8032	11.3734	13.0041	14.0432
49	1.2147	2.1489	4.9726	8.8029	11.3731	13.0036	14.0425
64	1.2144	2.1487	4.9724	8.8028	11.373	13.0035	14.0422
81	1.2143	2.1485	4.9723	8.8027	11.373	13.0034	14.0421

Table 3 Comparison study of the non-dimensional central deflection ($\bar{W} = 100wE_c h^3 / qa^4$) of a square SSSS symmetric ($0^\circ/90^\circ/\text{core}/90^\circ/0^\circ$) sandwich flat panel under the uniformly distributed loading

Model	$al/h = 50$			$al/h = 100$		
	$h_c/h_f = 2$	$h_c/h_f = 5$	$h_c/h_f = 8$	$h_c/h_f = 2$	$h_c/h_f = 5$	$h_c/h_f = 8$
Present	0.0114	0.0149	0.0234	0.0111	0.014	0.0206
FSDT [14]	0.01154	0.01593	0.02074	0.01145	0.01577	0.02052
TSDT [14]	0.0117	0.01672	0.02259	0.01149	0.01597	0.02098
ND [14]	0.01169	0.0167	0.02256	0.01148	0.01595	0.02095

Table 4 Comparison study of the non-dimensional fundamental frequency ($\varpi = (\omega b^2/h) \sqrt{(\rho/E_2)_f}$) of a square SSSS anti-symmetric ($0^\circ/90^\circ/\text{core}/0^\circ/90^\circ$) sandwich flat panel ($h_c/h_f = 10$)

al/h	Present	Kant and Swaminathan [9]	Kant and Swaminathan [9]	Reddy [1]	Senthilnathan et al. [2]
2	1.2151	1.1941	1.1734	1.6252	1.6252
4	2.1494	2.1036	2.0913	3.1013	3.1013
10	4.9729	4.8594	4.8519	7.0473	7.0473
20	8.8032	8.5955	8.5838	11.2664	11.2664
30	11.3734	11.0981	11.0788	13.664	13.664
40	13.0041	12.6821	12.6555	14.439	14.439
50	14.0432	13.6899	13.6577	15.0323	15.0323

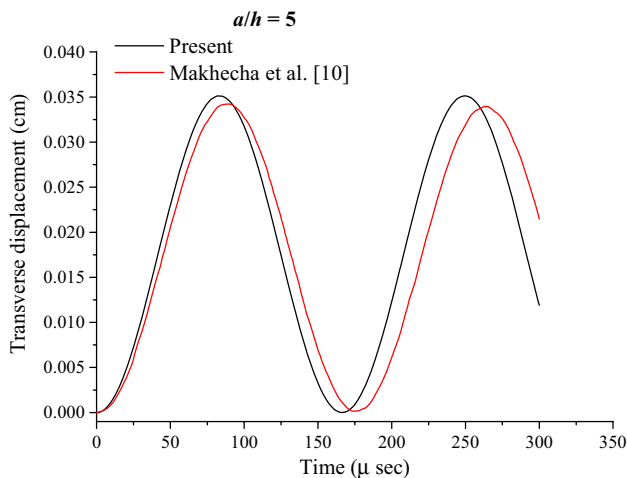


Fig. 5 Validation behaviour of transient responses of ($0^\circ/90^\circ/\text{core}/90^\circ/0^\circ$) a square SSSS sandwich flat panel under SSL ($al/h = 5$, $h_c/h_f = 8$)

including the similar geometrical parameter as in the convergence analysis, i.e., two span-to-thickness ratios ($al/h = 50$ and 100) and three core-to-face thickness ratios ($h_c/h_f = 2, 5$, and 8). The comparison between the present and reference deflection values are provided in Table 3. The comparison is showing good agreement with the published deflection values computed using the different theories.

Furthermore, the frequency validation has also been checked using the same problem as in the convergence test, i.e., a square SSSS anti-symmetric sandwich ($0^\circ/90^\circ/\text{core}/0^\circ/90^\circ$) plate structure the geometrical ($al/h = 2, 4, 10, 20, 30, 40$ and 50 and $h_c/h_f = 10$) and the material (M1) parameters as same as reference [9]. The results obtained using the current model and the reference frequencies are presented in Table 4. The comparison study indicates the accuracy of the derived model when compared with the frequencies computed via different mid-plane kinematic models.

Finally, the validation of transient deflection with the published results [10] is provided in Fig. 5. The required geometrical and the material properties including dimension are considered as same as the reference [10]. The time-dependent deflections of the square sandwich flat panel problem under the influence mechanical SSL ($q_0 = 100 \text{ N/cm}^2$) have been computed considering the input parameters as: SSSS, symmetric stacking sequence ($0^\circ/90^\circ/\text{core}/90^\circ/0^\circ$), $al/h = 5$ and $h_c/h_f = 8$. The figure indicates that the results are following good agreement with the reference with very small deviation [10] due to the type of kinematic theories.

3.1 Numerical illustrations

The different convergence and the validation studies indicate that the desired responses, i.e., the free vibration, static and time-dependent deflections of the curved/flat sandwich structures can be computed via the current higher order numerical model without affecting the accuracy. Now, several numerical examples are solved to display the applicability of the current higher order FE model for the different geometries (curved/flat) and design parameters. In general, the results are computed for the square sandwich curved/flat panels using the different combinations of end conditions (Fig. 2) and given elastic properties (Table 1), unless stated otherwise. Similarly, the total time including the time steps is taken for the transient analysis as 1 ms and $5 \mu\text{s}$, respectively, throughout the analysis.

3.1.1 Effect of the curvature ratios on the cylindrical shell panel

First, the central deflections parameters of square SSSS symmetric ($0^\circ/90^\circ/\text{core}/90^\circ/0^\circ$) cylindrical shell panel under two

Table 5 Effect of the curvature ratios on non-dimensional central deflections of a square SSSS (0°/90°/core/90°/0°) sandwich cylindrical shell panel ($h_c/h_f=20$)

R/a	Loading	a/h					
		5	20	30	50	80	100
2	UDL	0.6199	0.0644	0.0406	0.0237	0.0131	0.0094
5		0.6828	0.0771	0.0534	0.0394	0.0307	0.0265
10		0.6928	0.0793	0.0559	0.0434	0.0377	0.0354
20		0.6953	0.0799	0.0566	0.0445	0.0400	0.0386
50		0.6960	0.0801	0.0568	0.0448	0.0407	0.0396
2	SSL	0.4212	0.0428	0.0266	0.0154	0.0086	0.0062
5		0.4626	0.0509	0.0347	0.0251	0.0195	0.0168
10		0.4692	0.0523	0.0362	0.0276	0.0238	0.0223
20		0.4709	0.0527	0.0366	0.0283	0.0252	0.0243
50		0.4714	0.0528	0.0368	0.0285	0.0256	0.0249

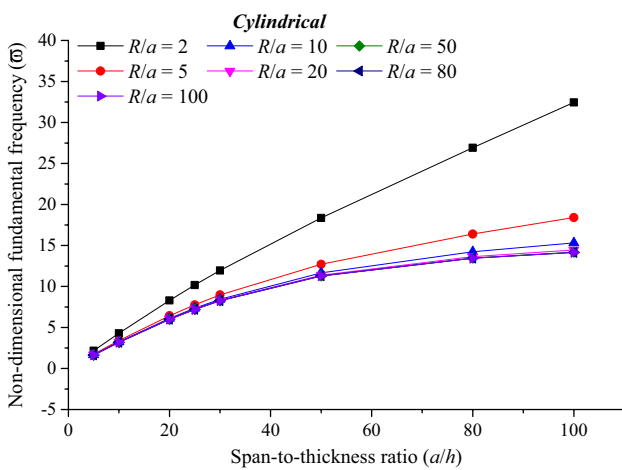


Fig. 6 Effect of curvature ratios on non-dimensional frequency responses of a square SSSS (0°/90°/Core/90°/0°) sandwich cylindrical shell panel ($h_c/h_f=20$)

different types of mechanical loading (UDL and SSL) deflections are computed for different curvature ratios ($R/a=2, 5, 10, 20,$ and 50) and are presented in Table 5. The desired structural parameters are evaluated including few more geometrical parameters, i.e., $a/h=5, 20, 30, 50, 80,$ and 100 and $h_c/h_f=20$. The tabulated deflection values indicate a decreasing slope for the higher span-to-thickness ratios (a/h), whereas a reverse trend for the curvature ratios (R/a). In addition, it can be noted that the deflections are higher for the UDL type of loading in comparison to the SSL. However, the magnitude of the UDL and SSL are same at peak. This is because the load intensities throughout the structural surface area remains same under the UDL but varies sinusoidally for the SSL.

Now, a square symmetric (0°/90°/core/90°/0°) cylindrical shell panel (SSSS) example problem has been solved using the structural input parameters as: $a/h=5, 10, 20, 25, 30, 50, 80,$ and 100 ; $R/a=2, 5, 10, 20, 50, 80,$ and 100 ; and $h_c/h_f=20$. Figure 6 shows the non-dimensional fundamental

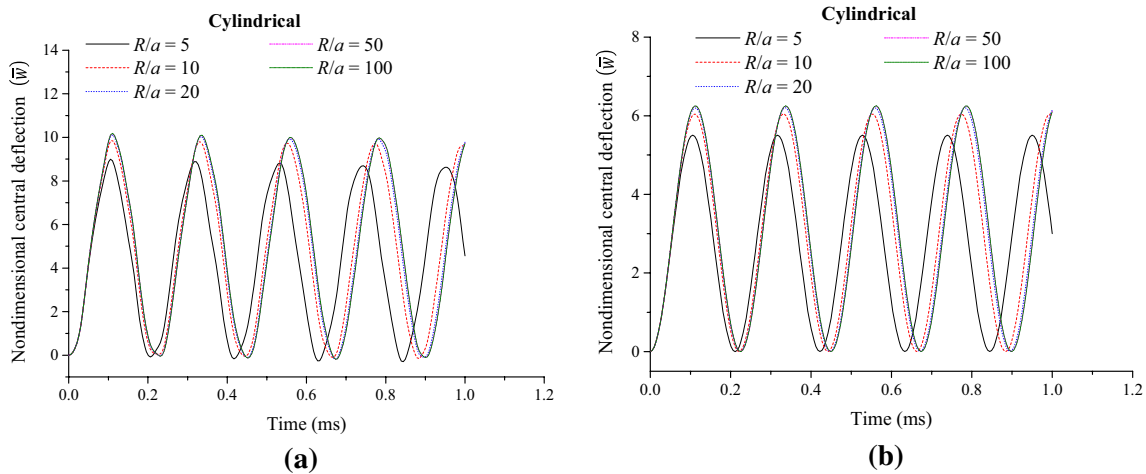


Fig. 7 Effect of curvature ratios on transient responses of a square SSSS (0°/90°/core/90°/0°) sandwich cylindrical shell panel under a UDL, b SSL ($a/h=50, h_c/h_f=20$)

frequency data. The variation of the vibration frequencies is following the expected line, i.e., increasing, while the span-to-thickness ratios increase but a declining trend for the higher curvature ratios.

Here, another example is solved to show the effect of the curvature ratios (R/a) on the transient responses of the cylindrical shell panel under the UDL and the SSL ($q_0 = 100 \text{ N/cm}^2$) type of loading and is presented in Fig. 7. To obtain the responses, a square SSSS symmetric ($0^\circ/90^\circ/\text{core}/90^\circ/0^\circ$) cylindrical sandwich shell panel is considered with $a/h = 50$ and $h_c/h_f = 20$. The results indicate that the deflection values are following an increasing trend when the curvature ratios (R/a) increase. However, the non-dimensional central deflection values (\bar{W}) are higher for the UDL in comparison to the SSL as discussed earlier.

3.1.2 Effect of the aspect ratios on the cylindrical shell panel

Now, the effect of the various aspect ratios on the transverse bending, frequency and transient deflections of the cylindrical panel examined in this example, similar to the earlier case. The non-dimensional transverse central point deflection parameters of a simply supported symmetric ($0^\circ/90^\circ/\text{core}/90^\circ/0^\circ$) cylindrical ($R/a = 10$) sandwich ($h_c/h_f = 20$) shell panel under two mechanical loadings (UDL and SSL) for various aspect ratios ($a/b = 0.5, 1.0, 1.5, 2.0$ and 3.0) are plotted in Fig. 8. In addition, the results are computed for the thick to thin structural panel considering six different span-to-thickness ratios ($a/h = 5, 20, 30, 50, 80$, and 100). The figure indicates the effect of both the geometrical parameters affect the deflections significantly, i.e., following a decreasing trend, while the aspect ratios and span-to-thickness ratio increase.

Now, the above example is extended to compute the eigenvalues of the cylindrical sandwich panel using the

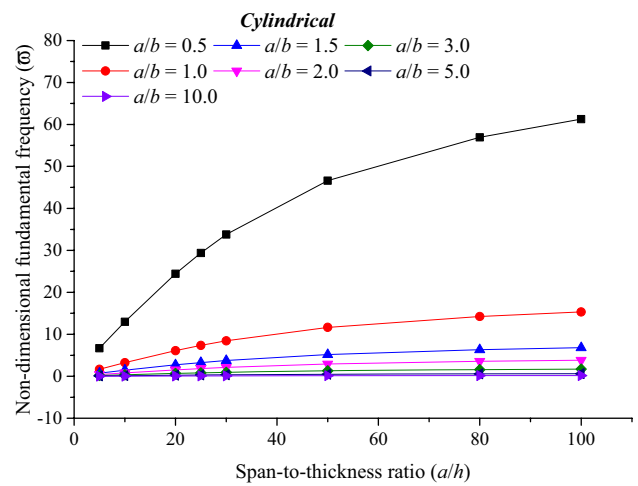


Fig. 9 Effect of aspect ratios on the non-dimensional central deflection of a SSSS ($0^\circ/90^\circ/\text{core}/90^\circ/0^\circ$) sandwich cylindrical shell panel ($R/a = 10, h_c/h_f = 20$)

similar input parameters and is plotted in Fig. 9. The responses follow the expected trend, i.e., the frequency values are decreasing, while the aspect ratios increase, whereas declining for the higher span-to-thickness ratios (a/h). In addition, the time-dependent deflections are computed for the same cylindrical sandwich shell example under the two different loadings as in the case of the deflection analysis, i.e., UDL and SDL, and are provided Fig. 10.

It is observed from the figure that the deflection parameter values (\bar{W}) follow a decreasing trend when the aspect ratios (a/b) increase. This is because of the non-dimensional formulae adopted in the current analysis. Furthermore, the similar kind of behaviour has been observed for the loading configurations (UDL and SDL) as same as the earlier case.

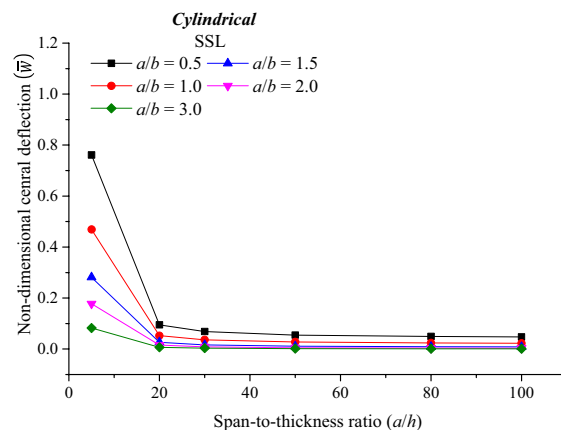
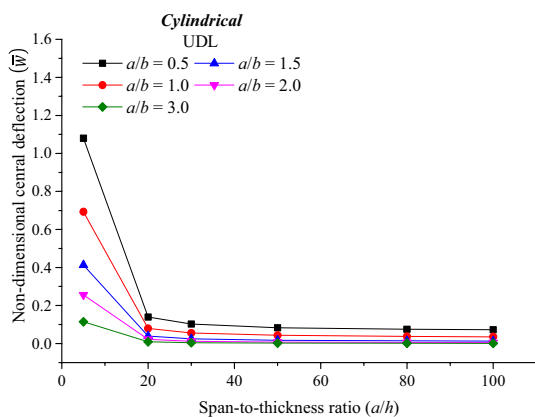


Fig. 8 Effect of aspect ratios on the non-dimensional central deflection of a SSSS ($0^\circ/90^\circ/\text{core}/90^\circ/0^\circ$) sandwich cylindrical shell panel ($R/a = 10, h_c/h_f = 20$)

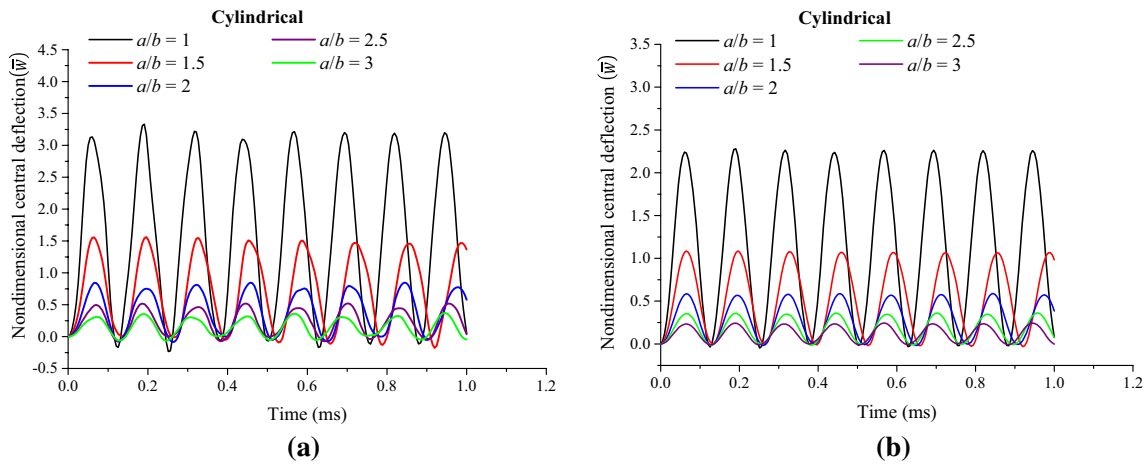


Fig. 10 Effect of aspect ratios on transient responses of a SSSS ($0^\circ/90^\circ/\text{core}/90^\circ/0^\circ$) sandwich cylindrical shell panel under **a** UDL, **b** SSL ($a/h=50, R/a=20, h_c/h_f=20$)

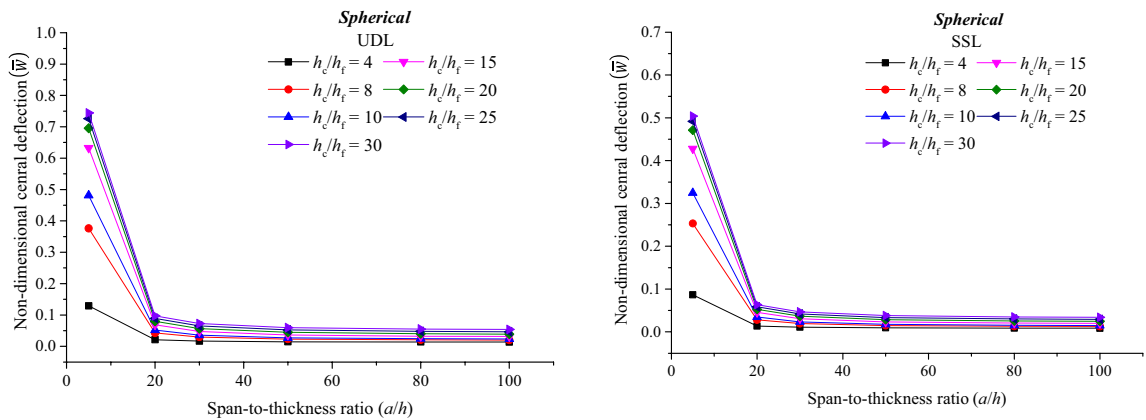


Fig. 11 Effect of core-to-face thickness ratios on the non-dimensional central deflection of a square SSSS ($0^\circ/90^\circ/\text{core}/90^\circ/0^\circ$) sandwich spherical shell panel ($R/a=10$)

3.1.3 Effect of the core-to-face thickness ratios on the spherical shell panel

In this section, the effect of the core-to-face thickness ratios ($h_c/h_f=4, 8, 10, 15, 20, 25,$ and 30) are investigated on the corresponding spherical ($R/a=10$) sandwich structural panel adopting the defined material and geometrical parameters. Figure 11 shows the deflection parameter of a square SSSS symmetric ($0^\circ/90^\circ/\text{core}/90^\circ/0^\circ$) sandwich spherical shell structure panel under the UDL and the SSL including the variable thickness ratios ($a/h=5, 20, 30, 50, 80,$ and 100). It can be easily understood from the figure that the deflection values are decreasing for the higher span-to-thickness ratios (a/h), whereas a reverse line followed, while the core-to-face thickness ratio increases. In addition, the present study also follows the similar type of behaviour as seen earlier for the loading condition (UDL and SSL).

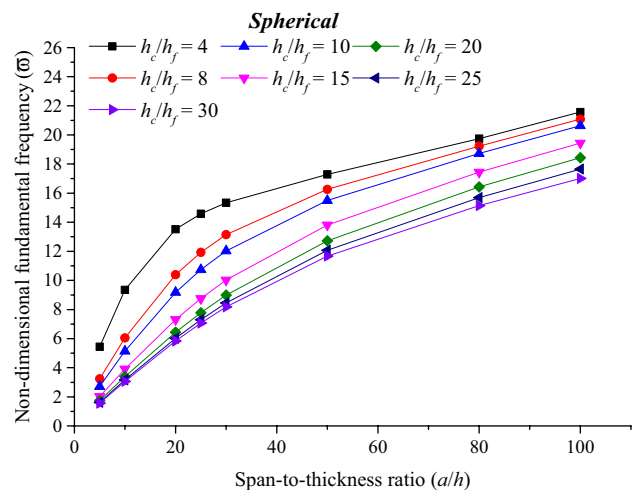


Fig. 12 Effect of core-to-face thickness ratios on non-dimensional frequency responses of a square SSSS ($0^\circ/90^\circ/\text{core}/90^\circ/0^\circ$) sandwich spherical shell panel ($R/a=10$)

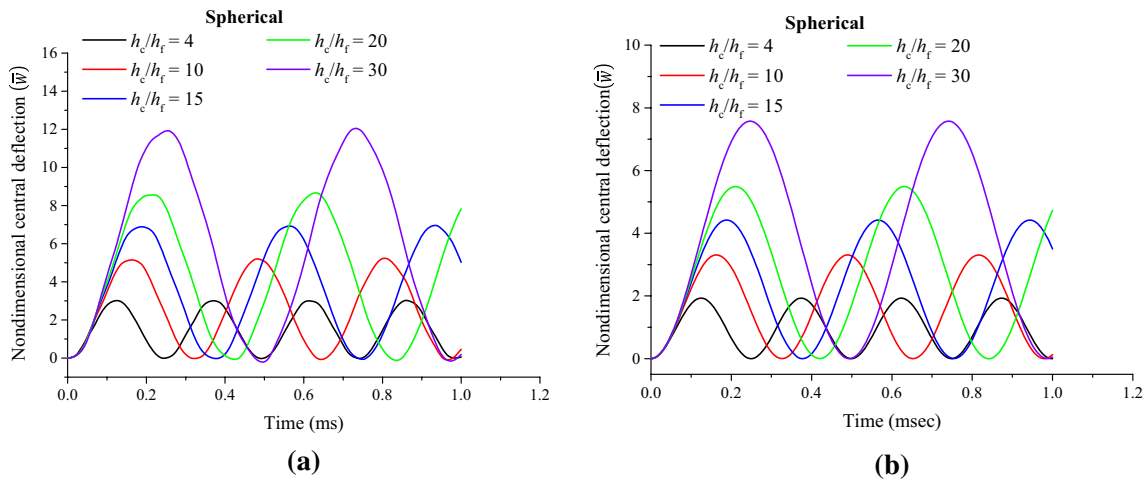


Fig. 13 Effect of core-to-face thickness ratios on transient responses of a square SSSS ($0^\circ/90^\circ/\text{core}/90^\circ/0^\circ$) sandwich spherical shell panel under **a** UDL, **b** SSL ($a/h=100$, $R/a=50$)

Table 6 Effect of the lamination scheme on the non-dimensional central deflection of a square SSSS sandwich hyperboloid shell panel ($R/a=10$, $h_c/h_f=20$)

Lamination scheme	Loading	ah					
		5	20	30	50	80	100
$0^\circ/\text{core}/0^\circ$	UDL	0.7592	0.0963	0.0647	0.0474	0.0413	0.0399
	SSL	0.5101	0.0635	0.0423	0.0308	0.0266	0.0257
$0^\circ/90^\circ/\text{core}/90^\circ/0^\circ$	UDL	0.6980	0.0803	0.0569	0.0450	0.0409	0.0399
	SSL	0.4724	0.0529	0.0368	0.0286	0.0258	0.0251
$0^\circ/90^\circ/0^\circ/90^\circ/\text{core}/90^\circ/0^\circ/90^\circ/0^\circ$	UDL	0.6963	0.0803	0.0569	0.0450	0.0409	0.0399
	SSL	0.4701	0.0529	0.0368	0.0286	0.0258	0.0251

Now, Fig. 12 shows the fundamental frequency parameter of a square symmetric ($0^\circ/90^\circ/\text{core}/90^\circ/0^\circ$) sandwich spherical panel for all sides simply supported. It is noticed from the provided data that the frequencies are following a declining path for the higher core-to-face thicknesses and a reverse trend when the span-to-thickness ratios (ah) increase.

Furthermore, the transient responses of a square SSSS symmetric ($0^\circ/90^\circ/\text{core}/90^\circ/0^\circ$) sandwich spherical shell panel under two different mechanical loading (UDL and SSL) is obtained and is presented in Fig. 13. For the computational purpose, the desired structural parameters are taken as: $h_c/h_f=4, 10, 15, 20$, and 30 , $a/h=100$, and $R/a=50$. The results indicate that the transient deflection values are showing an increasing trend with an increase in the core-to-face thickness ratios (h_c/h_f). It is important to mention that the results follows the same trend for the UDL and the SSL case as discussed earlier, i.e., the deflection values higher for the UDL while compared with the SSL.

Table 7 Effect of the lamination scheme on the non-dimensional fundamental frequency of a square SSSS sandwich hyperboloid shell panel ($R/a=10$, $h_c/h_f=20$)

ah	Lamination schemes		
	$0^\circ/\text{core}/0^\circ$	$0^\circ/90^\circ/\text{core}/90^\circ/0^\circ$	$0^\circ/90^\circ/0^\circ/90^\circ/\text{core}/90^\circ/0^\circ/90^\circ/0^\circ$
5	1.6337	1.6412	1.659
10	3.1181	3.1822	3.1918
20	5.6272	5.9836	5.9891
25	6.6743	7.1878	7.1924
30	7.606	8.2503	8.2544
50	10.41	11.2535	11.2562
80	12.7299	13.407	13.4086
100	13.5727	14.1082	14.1094

3.1.4 Effect of the lamination schemes on the hyperboloid shell panel

The effect of the face sheet laminations on the free vibration frequencies and static including the dynamic responses of the hyperboloid shell structure are discussed in this section. For

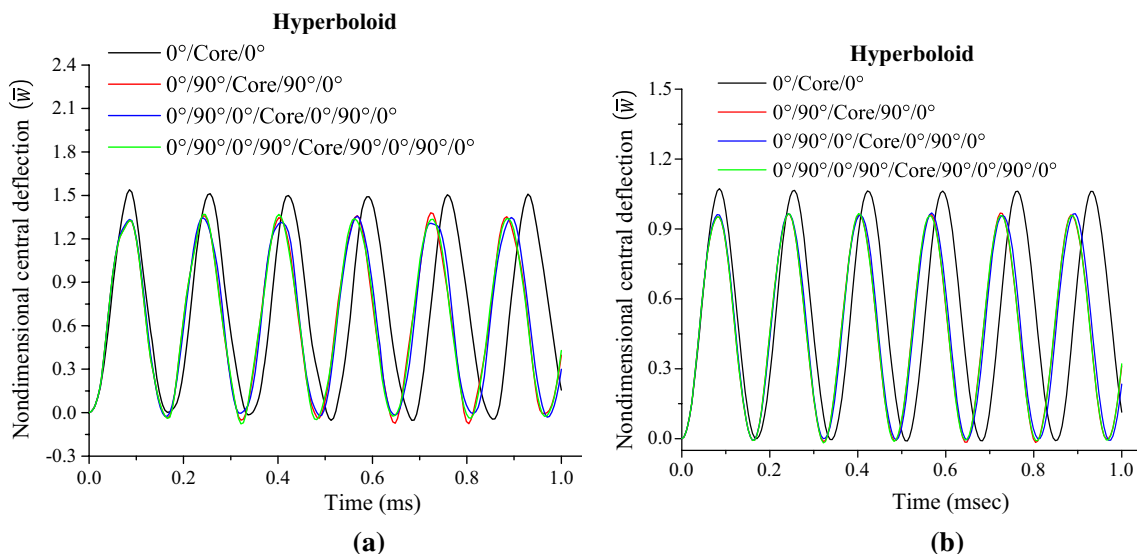


Fig. 14 Effect of lamination schemes on transient responses of a square CCCC sandwich hyperboloid shell panel under **a** UDL, **b** SSL ($a/h = 100, R/a = 50, h_c/h_f = 10$)

the analysis purpose, the geometrical and material parameters are taken as defined earlier. The numerical deflection responses of a square SSSS sandwich ($h_c/h_f = 20$) hyperboloid shell ($R/a = 10$) panel under the different mechanical loading (UDL and SSL) are solved to obtain the static responses and are presented in Table 6. For the computation purpose, three different lamination schemes are considered by varying the number of facesheets [(0°/core/0°), (0°/90°/core/90°/0°), and (0°/90°/0°/90°/core/90°/0°/90°/0°)] including $a/h = 5, 20, 30, 50, 80,$ and 100 . The results are showing a declining trend for the higher span-to-thickness ratios (a/h) and the number of facesheet layers. In addition, the deflections are higher for the UDL as same as the earlier examples.

Now, the frequency responses are obtained for a square SSSS sandwich hyperboloid shell panel of different lamination schemes and are presented in Table 7. For this numerical example, the desired structural parameters are taken as, $a/h = 5, 10, 20, 25, 30, 50, 80,$ and $100, h_c/h_f = 20,$ and $R/a = 10$. The results indicate that the non-dimensional eigenvalues are increasing when the span-to-thickness ratios (a/h) and the number of facesheet layers increase.

Now, the effect of lamination schemes on the transient responses of the clamped sandwich ($h_c/h_f = 10$) hyperboloid shell ($R/a = 50$) panel is computed under two mechanical loadings (UDL and SDL) including $a/h = 100$ and is presented in Fig. 14. From the results it can be visualize that the deflection values are decreasing when the numbers of face layers' increase. In addition, the final time-dependent deflections are following similar trend as in the earlier cases, i.e., higher for UDL while compared to the SDL.

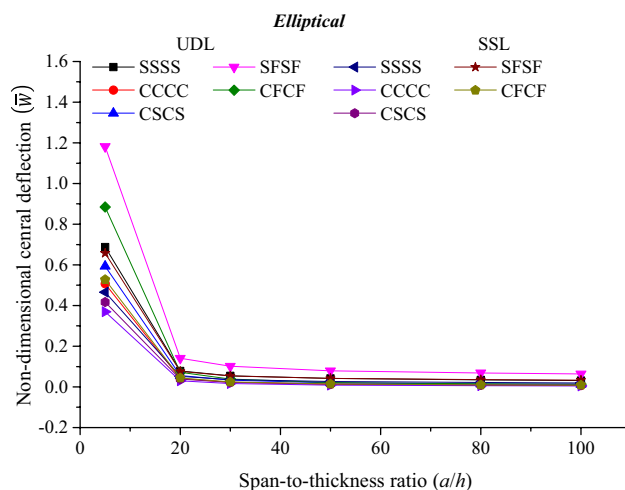


Fig. 15 Effect of support conditions on non-dimensional central deflections of a square (0°/90°/core/90°/0°) sandwich elliptical shell panel ($R/a = 10, h_c/h_f = 20$)

3.1.5 Effect of the support conditions on the elliptical shell panel

The effect of the different edge conditions (all edges simply supported, SSSS; all edges clamped, CCCC; two opposite edges simply supported and two free, SFSF; two opposite edges clamped and two free, CFCF; and two opposite edges clamped and two free, CSCS) on the static and dynamic deflections including the eigenvalue parameters are evaluated for the elliptical sandwich shell panel.

First, the deflection values are obtained for a square symmetric (0°/90°/core/90°/0°) sandwich elliptical shell panel

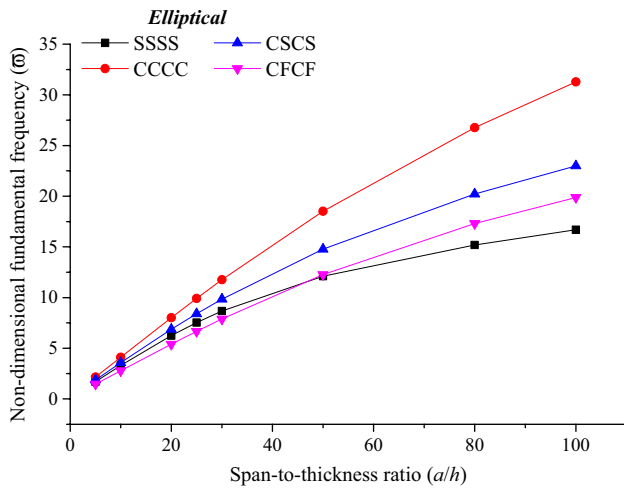


Fig. 16 Effect of support conditions on non-dimensional fundamental frequency responses of a square ($0^\circ/90^\circ/\text{core}/90^\circ/0^\circ$) sandwich elliptical shell panel ($R/a = 10, h_c/h_f = 20$)

and are presented in Fig. 15. The results are computed for the various edge condition as mentioned above under the UDL and the SSL by considering the structural parameters as, $a/h = 5, 20, 30, 50, 80,$ and $100, h_c/h_f = 20,$ and $R/a = 10$. It is noticed from the data that the responses are following the similar type of trend as seen in the earlier sections. It is also observed that the deflection values are following the decreasing trend with the change in the edge conditions from SFSF, CFCF, SSSS, CSCS, and CCCC.

Now, the example is extended to investigate frequency parameters of the sandwich elliptical shell panel and is presented in Fig. 16. For the computational purpose, the desired structural parameters are adopted as: $a/h = 5, 10,$

$20, 25, 30, 50, 80,$ and $100, h_c/h_f = 20,$ and $R/a = 10$. The responses indicate that the frequency values are increasing when the span-to-thickness ratios (a/h) increase. In addition, the clamped panel is showing the higher frequency parameters when compared to the other support conditions.

Furthermore, the effect of the predefined end conditions on the transient responses of a square sandwich elliptical shell panel is analysed under the two different type of mechanical loading, i.e., the UDL and the SSL and is presented in Fig. 17. The responses are computed using the desired structural parameters as, $a/h = 50, R/a = 100, h_c/h_f = 20$. It is noticed from the responses that the deflection values are following a decreasing type of trend when the support changes from, SFSF, SSSS, CFCF, CSCS, and CCCC, progressively.

3.1.6 Responses of the different shell panels

Finally, the effect of the geometrical configuration on the corresponding eigenvalues and static including the dynamic deflections are investigated utilizing the predefined input geometrical and material parameters. The non-dimensional central deflection parameters of a square SSSS symmetric ($0^\circ/90^\circ/\text{core}/90^\circ/0^\circ$) sandwich shell panel are obtained and are tabulated in Table 8. The responses are calculated using the same material and geometrical parameters as discussed earlier under the influence of the UDL and the SSL. For the computational purpose, the necessary structural parameters are taken as, $a/h = 5, 20, 30, 50, 80,$ and $100, h_c/h_f = 20,$ and $R/a = 10$. As discussed in earlier cases, the responses are following the similar type of trend, i.e., the deflection values are decreasing when the span-to-thickness ratios (a/h)

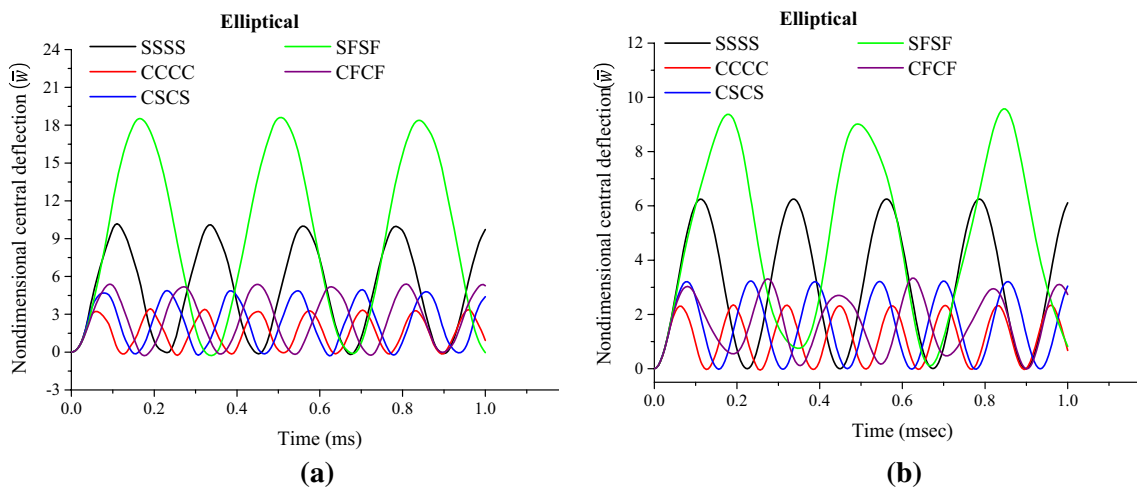


Fig. 17 Effect of support conditions on transient responses of ($0^\circ/90^\circ/\text{core}/90^\circ/0^\circ$) sandwich elliptical shell panel under **a** UDL, **b** SSL ($a/h = 50, R/a = 100, h_c/h_f = 20$)

Table 8 Non-dimensional central deflection responses of a square SSSS symmetric (0°/90°/core/90°/0°) sandwich shell panels ($R/a = 10, h_c/h_f = 20$)

Type of shell	Loading	a/h					
		5	20	30	50	80	100
Flat	UDL	0.6961	0.0801	0.0568	0.0449	0.0408	0.0398
	SSL	0.4714	0.0528	0.0368	0.0286	0.0257	0.0251
Cylindrical	UDL	0.6928	0.0793	0.0559	0.0434	0.0377	0.0354
	SSL	0.4692	0.0523	0.0362	0.0276	0.0238	0.0223
Spherical	UDL	0.6808	0.0769	0.0533	0.0393	0.0306	0.0264
	SSL	0.4616	0.0508	0.0346	0.0251	0.0195	0.0168
Hyperboloid	UDL	0.6980	0.0803	0.0569	0.0450	0.0409	0.0399
	SSL	0.4724	0.0529	0.0368	0.0286	0.0258	0.0251
Elliptical	UDL	0.6875	0.0783	0.0548	0.0415	0.0344	0.0310
	SSL	0.4659	0.0516	0.0355	0.0265	0.0218	0.0196

Table 9 Non-dimensional fundamental frequency responses of a square (0°/90°/core/90°/0°) simply supported sandwich shell panels ($R/a = 10, h_c/h_f = 20$)

a/h	Flat	Cylindrical	Spherical	Hyperboloid	Elliptical
5	1.6445	1.6694	1.7454	1.6412	1.7018
10	3.1886	3.2404	3.397	3.1822	3.3072
20	5.9956	6.1063	6.4385	5.9836	6.2481
25	7.2021	7.3466	7.7775	7.1878	7.5306
30	8.2668	8.4486	8.9874	8.2503	8.6788
50	11.2757	11.6492	12.7235	11.2535	12.1106
80	13.4329	14.2351	16.4282	13.4070	15.1901
100	14.1349	15.3177	18.4345	14.1082	16.6902

increase. In addition, the deflections are higher for the UDL in comparison to the SSL as seen in the earlier examples. Furthermore, the transverse central deflection parameters are decreasing in progressive manner when the geometry

changes from hyperboloid, flat, cylindrical, elliptical and spherical panel.

Table 9 reports the frequency responses for the different geometrical configurations of the square SSSS symmetric (0°/90°/core/90°/0°) sandwich panels. The structural responses are obtained by setting the geometrical parameters as: $a/h = 5, 10, 20, 25, 30, 50, 80,$ and $100, h_c/h_f = 20,$ and $R/a = 10$. The frequency responses show an increasing type of trend when the span-to-thickness ratios increase as seen in the earlier examples. The frequency values are higher for and lower for the spherical and hyperboloid panel configurations.

Now, the transient responses of various sandwich shell geometries (flat, cylindrical, elliptical, spherical and hyperboloid) under the influence of two loading types (UDL and SSL) computed using the current higher order model and are plotted in Fig. 18. The central deflection parameter (\bar{W}) of the clamped sandwich shell panels are computed using the relevant input parameters as: $a/h = 50,$

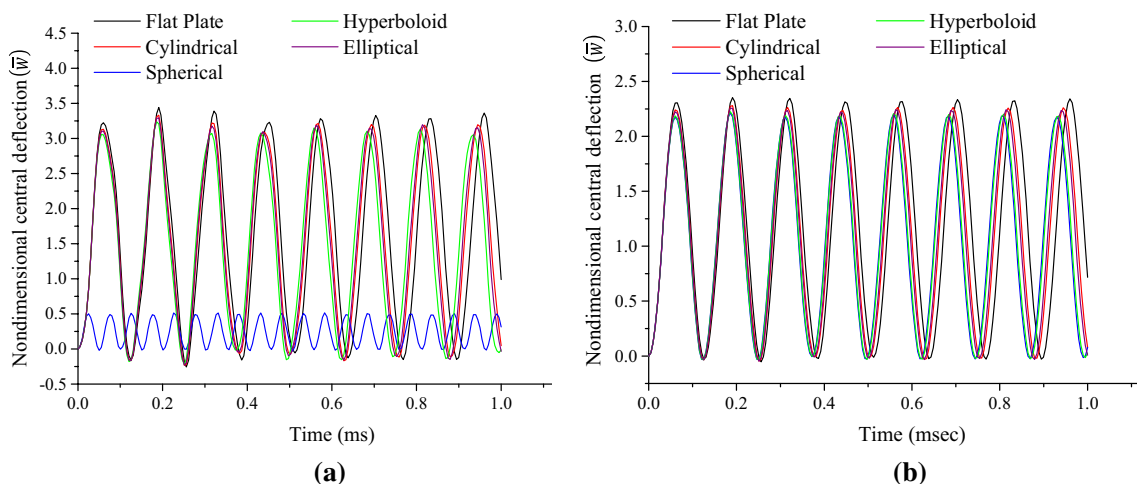


Fig. 18 Transient responses of a square (0°/90°/core/90°/0°) clamped sandwich shell panels under **a** UDL, **b** SSL ($a/h = 50, R/a = 20, h_c/h_f = 20$)

$R/a=20$ and $h_c/h_f=20$. The deflections are higher for the UDL in comparison to SSL. However, the peaks are same in both the loading cases but higher deflections observed in the UDL. This is because the distribution of loading intensity throughout the panel surface area same for the UDL, whereas it varies sinusoidally for the SSL case and the deflection follows the path accordingly.

4 Conclusions

The FE solutions of structural responses, i.e., the static and the dynamic deflection including the free vibration frequencies of the layered sandwich curved structures are computed using the proposed higher order mathematical model. The results are obtained using an own home-made customized MATLAB code with the help of defined geometrical and material parameters. The solution accuracy and the corresponding consistencies of the current output are demonstrated via validating the results with that of available published data and the convergence test. The comparison of results indicate that the current higher order polynomial kinematic model is sufficient to investigate the sandwich laminated flat/curved panel structures without increasing the computational cost. In addition, the model is extended further to compute the values (deflection, frequency and time-dependent deflection) via a series of numerical examples including the variable parameters associated with geometrical dimensions and configurations. Finally, the final understanding related to the current output data displayed in a pointwise fashion in the following lines.

- The free vibration non-dimensional frequency values are increasing, while the span-to-thickness ratios and the number of facings increase, whereas the trend follows a declined path for the aspect ratios, the curvature ratios, and the core-to-face thickness ratios
- Similarly, the non-dimensional central transverse deflection values are increasing for the higher curvature ratios and the core-to-face thickness ratios. However, a declining trend is observed, while the span-to-thickness ratios, the aspect ratios and the number of face sheets increase.
- Likewise, the deflection responses computed under two kinds of loading indicate that the non-dimensional central deflection values are higher under the influence of mechanical UDL instead of the SSL.
- Finally, the significance of the support conditions are indicative for each type of analysis (static and deflection including free vibration frequencies) irrespective of geometries and geometrical parameters.

References

1. Reddy JN (1984) A simple higher order theory for laminated composite plates. *ASME J Appl Mech* 51:745–752
2. Senthilnathan NR, Lim KH, Lee KH, Chow ST (1987) Buckling of shear deformable plates. *AISS J* 25(9):1268–1271
3. Kant T, Mallikarjuna B (1989) Transient dynamics of composite sandwich plates using 4-, 8-, 9-noded isoparametric quadrilateral elements. *Finite Elem Anal Des* 6:307–318
4. Kant T, Arora CP, Varaiya JH (1990) Finite element transient analysis of composite and sandwich plates based on a refined theory and a mode superposition method. *Comput Struct* 22(2):109–120
5. Kant T, Varaiya JH, Arora CP (1992) Finite element transient analysis of composite and sandwich plates based on a refined theory and implicit time integration schemes. *Compos Struct* 36(3):401–420
6. Kommineni JR, Kant T (1993) Large deflection elastic and inelastic transient analyses of composite and sandwich plates with a refined theory. *J Reinf Plast Compos* 12:1150–1170
7. Kant T, Kommineni JR (1994) Geometrically non-linear transient analysis of laminated composite and sandwich shells with a refined theory and C^0 finite elements. *Comput Struct* 52:1243–1259
8. Kommineni JR, Kant T (1995) Pseudo-transient large deflection analysis of composite and sandwich shells with a refined theory. *Comput Methods Appl Mech Eng* 123:1–13
9. Kant T, Swaminathan K (2001) Analytical solutions for free vibration of laminated composite and sandwich plates based on a higher-order refined theory. *Compos Struct* 53:73–85
10. Makhecha DP, Patel BP, Ganapathi M (2001) Transient dynamics of thick skew sandwich laminates under thermal/mechanical loads. *J Reinf Plast Compos* 20:1524–1545
11. Nayak AK, Sheno RA, Moy SSSJ (2002) Transient analysis of composite sandwich plates using assumed strain plate bending elements based on Reddy's higher order theory. *Adv Polym Compos Struct Appl Constr* 216:347–357. ISBN 978-1-85573-736-5
12. Nayak AK, Sheno RA, Moy SSSJ (2004) Transient response of composite sandwich plates. *Compos Struct* 64:249–267
13. Roque CMC, Ferreira AJM, Neves AMA, Soares CMM, Reddy JN, Jorge RMN (2011) Transient analysis of composite and sandwich plates by radial basis functions. *J Sandw Struct Mater* 13:681–704
14. Madhukar S, Singha MK (2013) Geometrically nonlinear finite element analysis of sandwich plates using normal deformation theory. *Compos Struct* 97:84–90
15. Ferreira AJM, Viola E, Tornabene F, Fantuzzi N, Zenkour AM (2013) Analysis of sandwich plates by generalized differential quadrature method. *Math Probl Eng* 2013:1–12. <https://doi.org/10.1155/2013/964367>
16. Marjanović M, Vuksanović D (2014) Transient analysis of laminated composite and sandwich plates with embedded delaminations using GLPT. In: *Proc. 9th int conf struct Dyn Porto*, pp 3373–3380
17. Marjanović M, Vuksanović D, Meschke G (2015) Geometrically nonlinear transient analysis of delaminated composite and sandwich plates using a layerwise displacement model with contact conditions. *Compos Struct* 122:67–81
18. Qu Y, Wu S, Li H, Meng G (2015) Three-dimensional free and transient vibration analysis of composite laminated and sandwich rectangular parallelepipeds: Beams, plates and solids. *Compos Part B Eng* 73:96–110
19. Mishra PK, Pradhan AK, Pandit MK (2016) Inter-laminar delamination analyses of spar wingskin joints made with flat FRP composite laminates. *Int J Adhes Adhes* 68:19–29
20. Yin S, Yu T, Bui TQ, Liu P, Hirose S (2016) Buckling and vibration extended isogeometric analysis of imperfect graded

- Reissner-Mindlin plates with internal defects using NURBS and level sets. *Comput Struct* 177:23–38
21. Nguyen MN, Bui TQ, Truong TT, Tanaka S, Hirose S (2017) Numerical analysis of 3-D solids and composite structures by an enhanced 8-node hexahedral element. *Finite Elem Anal Des* 131:1–16
 22. Tornabene F, Fantuzzi N, Baccocchi M, Viola E, Reddy JN (2017) A numerical investigation on the natural frequencies of FGM sandwich shells with variable thickness by the local generalized differential quadrature method. *Appl Sci* 7(131):1–39
 23. Tornabene F, Fantuzzi N, Baccocchi M, Reddy JN (2017) An equivalent layer-wise approach for the free vibration analysis of thick and thin laminated and sandwich shells. *Appl Sci* 7(17):1–34
 24. Tornabene F, Brischetto S (2018) 3D capability of refined GDQ models for the bending analysis of composite and sandwich plates, spherical and doubly-curved shells. *Thin Walled Struct* 129:94–124
 25. Szekrényes A (2017) Analytical solution of some delamination scenarios in thick structural sandwich plates. *J Sandw Struct Mater*. <https://doi.org/10.1177/1099636217714182>
 26. Szekrényes A (2018) The role of transverse stretching in the delamination fracture of softcore sandwich plates. *Appl Math Model* 63:611–632
 27. Heydari MM, Kolahchi R, Heydari M, Abbasi A (2014) Exact solution for transverse bending analysis of embedded laminated Mindlin plate. *Struct Eng Mech* 49(5):661–672
 28. Bidgoli AMM, Daneshmehr AR, Kolahchi R (2015) Analytical bending solution of fully clamped orthotropic rectangular plates resting on elastic foundations by the finite integral transform method. *J Appl Comput Mech* 1(2):52–58
 29. Kolahchi R (2017) A comparative study on the bending, vibration and buckling of viscoelastic sandwich nano-plates based on different nonlocal theories using DC, HDQ and DQ methods. *Aerosp Sci Technol* 66:235–248
 30. Arani AG, Jafari SS, Kolahchi R (2017) Nonlinear vibration analysis of viscoelastic micro nano-composite sandwich plates integrated with sensor and actuator. *Microsyst Technol* 23(5):1509–1535
 31. Kolahchi R, Bidgoli AMM (2016) Size-dependent sinusoidal beam model for dynamic instability of single walled carbon nanotubes. *Appl Math Mech* 37(2):265–274
 32. Kolahchi R, Zarei MS, Hajmohammad MH, Nouri A (2017) Wave propagation of embedded viscoelastic FG-CNT-reinforced sandwich plates integrated with sensor and actuator based on refined Zigzag theory. *Int J Mech Sci*. <https://doi.org/10.1016/j.ijmecsci.2017.06.039>
 33. Zarei MS, Hajmohammad MH, Kolahchi R, Karami H (2018) Dynamic response control of aluminum beams integrated with nanocomposite piezoelectric layers subjected to blast load using hyperbolic visco-piezo-elasticity theory. *J Sandw Struct Mater*. <https://doi.org/10.1177/1099636218785316>
 34. Hajmohammad MH, Farrokhanian A, Kolahchi R (2018) Smart control and vibration of viscoelastic actuator-multiphase nanocomposite conical shells-sensor considering hygrothermal load based on layerwise theory. *Aerosp Sci Technol*. <https://doi.org/10.1016/j.ast.2018.04.030>
 35. Hajmohammad MH, Azizkhani MB, Kolahchi R (2018) Multiphase nanocomposite viscoelastic laminated conical shells subjected to magneto-hygrothermal loads: Dynamic buckling analysis. *Int J Mech Sci*. <https://doi.org/10.1016/j.ijmecsci.2018.01.026>
 36. Bessaim A, Houari MSA, Tounsi A, Mahmoud SR, Bedia EAA (2013) A new higher-order shear and normal deformation theory for the static and free vibration analysis of sandwich plates with functionally graded isotropic face sheets. *J Sandw Struct Mater* 15(6):671–703
 37. Mahi A, Bedia EAA, Tounsi A (2015) A new hyperbolic shear deformation theory for bending and free vibration analysis of isotropic, functionally graded, sandwich and laminated composite plates. *Appl Math Model* 39:2489–2508
 38. Abualnour M, Houari MSA, Tounsi A, Bedia EAA, Mahmoud SR (2018) A novel, quasi-3D trigonometric plate theory for free vibration analysis of advanced composite plates. *Compos Struct* 184:688–697
 39. Bousahla AA, Houari MSA, Tounsi A, Bedia EAA (2014) A novel higher order shear and normal deformation theory based on neutral surface position for bending analysis of advanced composite plates. *Int J Comput Methods* 11(6):1350082
 40. Meziene MAA, Abdelaziz HH, Tounsi A (2014) An efficient and simple refined theory for buckling and free vibration of exponentially graded sandwich plates under various boundary conditions. *J Sandw Struct Mater* 16(3):293–318
 41. Hamidi A, Houari MSA, Mahmoud SR, Tounsi A (2015) A sinusoidal plate theory with 5-unknowns and stretching effect for thermomechanical bending of functionally graded sandwich plates. *Steel Compos Struct* 18(1):235–253
 42. Yahia SA, Atmane HA, Houari MSA, Tounsi A (2015) Wave propagation in functionally graded plates with porosities using various higher-order shear deformation plate theories. *Struct Eng Mech* 53(6):1143–1165
 43. Bellifa H, Benrahou KH, Hadji L, Houari MSA, Tounsi A (2016) Bending and free vibration analysis of functionally graded plates using a simple shear deformation theory and the concept the neutral surface position. *J Braz Soc Mech Sci Eng* 38:265–275
 44. Bennoun M, Houari MSA, Tounsi A (2016) A novel five variable refined plate theory for vibration analysis of functionally graded sandwich plates. *Mech Adv Mater Struct* 23(4):423–431
 45. Boudarba B, Houari MSA, Tounsi A, Mahmoud SR (2016) Thermal stability of functionally graded sandwich plates using a simple shear deformation theory. *Struct Eng Mech* 58(3):397–422
 46. Abdelaziz HH, Meziene MAA, Bousahla AA, Tounsi A, Mahmoud SR, Alwabri AS (2017) An efficient hyperbolic shear deformation theory for bending, buckling and free vibration of FGM sandwich plates with various boundary conditions. *Steel Compos Struct* 25(6):693–704
 47. Bouafia K, Kaci A, Houari MSA, Benzair A, Tounsi A (2017) A nonlocal quasi-3D theory for bending and free flexural vibration behaviors of functionally graded nanobeams. *Smart Struct Syst* 19(2):115–126
 48. El-Haina F, Bakora A, Bousahla AA, Tounsi A, Mahmoud SR (2017) A simple analytical approach for thermal buckling of thick functionally graded sandwich plates. *Struct Eng Mech* 63(5):585–595
 49. Menasria A, Bouhadra A, Tounsi A, Bousahla AA, Mahmoud SR (2017) A new and simple HSDT for thermal stability analysis of FG sandwich plates. *Steel Compos Struct* 25(2):157–175
 50. Belabed Z, Bousahla AA, Houari MSA, Tounsi A, Mahmoud SR (2018) A new 3-unknown hyperbolic shear deformation theory for vibration of functionally graded sandwich plate. *Earthq Struct* 14(2):103–115
 51. Bouhadra A, Tounsi A, Bousahla AA, Benyoucef S, Mahmoud SR (2018) Improved HSDT accounting for effect of thickness stretching in advanced composite plates. *Struct Eng Mech* 66(1):61–73
 52. Karami B, Janghorban M, Shahsavari D, Tounsi A (2018) A size-dependent quasi-3D model for wave dispersion analysis of FG nanoplates. *Steel Compos Struct* 28(1):99–110
 53. Karami B, Janghorban M, Tounsi A (2018) Variational approach for wave dispersion in anisotropic doubly-curved nanoshells based on a new nonlocal strain gradient higher order shell theory. *Thin Walled Struct* 129:251–264

54. Younsi A, Tounsi A, Zaoui FZ, Bousahla AA, Mahmoud SR (2018) Novel quasi-3D and 2D shear deformation theories for bending and free vibration analysis of FGM plates. *Geomech Eng* 14(6):519–532
55. Zine A, Tounsi A, Draiche K, Sekkal M, Mahmoud SR (2018) A novel higher-order shear deformation theory for bending and free vibration analysis of isotropic and multilayered plates and shells. *Steel Compos Struct* 26(2):125–137
56. Katariya PV, Hirwani CK, Panda SK (2018) Geometrically non-linear deflection and stress analysis of skew sandwich shell panel using higher-order theory. *Eng Comput*. <https://doi.org/10.1007/s00366-018-0609-3>
57. Jones RM (1999) *Mechanics of composite materials*. Taylor & Francis, Philadelphia
58. Cook RD, Malkus DS, Plesha ME, Witt RJ (2003) *Concepts and applications of finite element analysis*. Wiley, Singapore
59. Bathe KJ, Ramm E, Wilson EL (1975) Finite-element formulations for large deformation dynamic analysis. *Int J Numer Methods Eng* 9:353–386

Publisher's Note Springer Nature remains neutral with regard to jurisdictional claims in published maps and institutional affiliations.